Proc. Natl. Acad. Sci. USA
Vol. 76, No. 11, pp. 5650–5654, November 1979
Biophysics

Rotational diffusion of cell surface components by time-resolved phosphorescence anisotropy

(eosin/triplet probe/polarization/anion transport/lectin receptors)

ROBERT H. AUSTIN*, SHIRLEY SUILING CHAN†, AND THOMAS M. JOVIN‡

Abteilung Molekulare Biologie, Max Planck Institut für Biophysikalische Chemie, Postfach 968, D-34 Göttingen, West Germany

Communicated by Manfred Eigen, August 8, 1979

ABSTRACT **The rotational diffusion of concanavalin A receptors of viable Friend erythroleukemia cells and the band 3 anion transport system of human erythrocytes has been measured via the time-dependent phosphorescence emission intensity and anisotropy of triplet probes excited by a 5-ns laser pulse. High-quality phosphorescence decay curves with a 1-μs time resolution were obtained at concentrations of the eosin probe down to 20 nM and in aqueous media at temperatures of 4–38°C. A strong temperature dependence in the rotational behavior was observed for the band 3 anion transport protein, but the lectin receptors of the Friend erythroleukemia cells were found to be immobile on the time scale of 1–4000 μs at either 4°C or 37°C. The technique is applicable to other triplet probes and membrane components of living cells under conditions that do not destroy viability.**

The rotational diffusion of macromolecules reflects the combined effects of (*i*) size, shape, and internal flexibility, (*ii*) environmental fluidity and stereochemical constraints, and (*iii*) static and dynamic interactions with other molecules. The techniques of steady-state (1), phase-shift (2), and time-resolved (3, 4) fluorescence depolarization have been applied extensively to studies in fluid media but are limited by typical fluorescence lifetimes (<0.1 μs) and the viscosity of aqueous solutions [≈1 cP (1 P = 0.1 Pa·s)] to rigid molecules smaller than 10^6 daltons. In the case of larger oligomeric macromolecules and assemblies, or of rotation in viscous media—e.g., biological membranes—methods with a longer time range (>1 μs) are required (5).

There exists increasing evidence that the dynamic (diffusional) properties and aggregation states of cell surface components are correlated with cellular function such as metabolism, differentiation, transport, hormonal regulation, motion, and adhesion (6–9). Fluorescence methods have been applied extensively in studies of membrane dynamics (for a review see ref. 7). However, time-resolved rotational diffusion measurements on intact cells have not been reported.

A recent technique with the required temporal resolution exploits transient dichroic absorption changes due to the long-lived excited triplet state induced by the photoselective action of plane-polarized light (10). Rotational depolarization measurements using the anisotropic ground state depletion or triplet–triplet absorption signals of triplet states with millisecond lifetimes have been reported (and are reviewed in ref. 11). The essential limitation of the techniques based upon absorption is that of sensitivity. Signal-to-noise considerations (12) limit experiments to solutions or suspensions with concentrations of the triplet probe of at least 1–10 μM. This circumstance restricts the applicability of absorption dichroism to relatively few natural or *in vitro* membrane systems (6, 7, 11, 13). In particular, suspensions of most cells cannot be employed at the required densities without introducing unacceptable depolarization due to scattering.

We describe here a variation of the triplet probe approach that extends the sensitivity into the nanomolar range and is thus applicable to studies of living cells. It exploits the polarized *emission* properties of the triplet state—i.e., *time-resolved phosphorescence anisotropy in fluid media.*

MATERIALS AND METHODS

Eosin-Labeled Human Erythrocyte Ghosts. Erythrocytes from freshly drawn human blood were labeled with eosin 5′-isothiocyanate (EITC; Molecular Probes) according to Nigg *et al.* (14). The externally labeled ghosts produced after lysis and washing were suspended in 5 mM Na phosphate buffer, pH 7.3, and stored under argon at 4°C in the dark.

Eosin-Labeled Concanavalin A (Eosin-Con A). Jack bean concanavalin A (Con A) was the product of Sigma Chemicals. It was labeled with EITC under reduced light conditions (14) according to a procedure described elsewhere (15) for fluorescein isothiocyanate. The average labeling ratio was 1.2 eosin molecules per Con A tetramer, as determined by using an ϵ for eosin at 522 nm of 8.3×10^4 M^{-1} cm^{-1} (11).

Cells Labeled with Eosin-Con A. Friend virus-transformed mouse erythroleukemia cells (F4N line; ref. 16) suspended in cold phosphate-buffered saline (P_i/NaCl) were labeled for 30 min at 4°C with eosin-Con A at a saturating concentration of 200 μg/ml (17). The cells were washed with cold P_i/NaCl and adjusted to $8–10 \times 10^6$ cells per ml, equivalent to an eosin concentration of approximately 0.1 μM.

Time-Resolved Phosphorescence. See Fig. 1. A N_2 laser (Lambda Physik) operated at 2 mJ/pulse and 10 Hz drives a courmarin 307 dye laser so as to produce 150-μJ, 5-ns pulses at 500 nm. The light pulses pass through a polarizer and a static polarization rotator to the sample (approximately 300 μl) in a thermostated 5 × 5 mm quartz cuvette. The luminescence is collected at 90° (the rear face of the cuvette is aluminized externally) and the phosphorescence is isolated by a combination of KV550 and RG695 Schott filters. The two polarized emission components are detected in sequence by 90° rotations of a Polaroid sheet polarizer after every 32nd pulse. This is accomplished in 0.5 s by a stepping motor under microprocessor (Intel 8085) control and has the effect of canceling laser amplitude and other system fluctuations. The photomultiplier (EMI 9817 QGB) has an S20 cathode and a gating electrode. The latter is used to turn on the tube about 1 μs after the laser

Abbreviations: EITC, eosin 5′-isothiocyanate; Con A, concanavalin A; P_i/NaCl, phosphate-buffered saline.

* Present address: Department of Physics, Princeton University, Princeton, NJ 08540.
† Present address: Corporate Pioneering Research Laboratories, Exxon Research and Engineering Company, Linden, NJ 07036.
‡ To whom reprint requests should be addressed.

The publication costs of this article were defrayed in part by page charge payment. This article must therefore be hereby marked "*advertisement*" in accordance with 18 U. S. C. §1734 solely to indicate this fact.

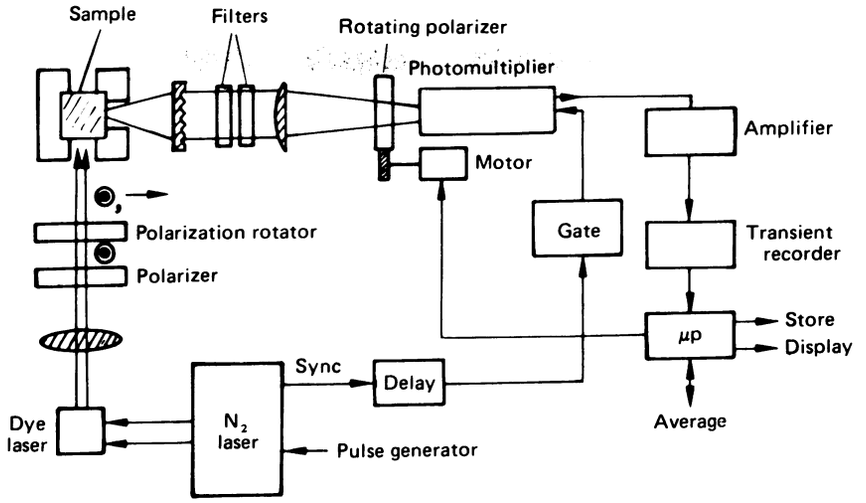

FIG. 1. Phosphorimeter. μp, Microprocessor.

pulse, thereby protecting the photomultiplier from the intense spike of prompt fluorescence. The signal is amplified with a bandwidth of generally 0.1 MHz and digitized with a Biomation 8100 transient recorder. The minimum sampling interval is 1 μs per point due to the gating of the photomultiplier and stray long-lived emission from the filters, which must be carefully chosen. Signal averaging is under microprocessor control and involves transfer to a Fabritek 1070 signal averager.

Triplet Absorption Measurements. Linear dichroism measurements with a temporal resolution of 10 ns were made in the same apparatus (Fig. 1) equipped with a He–Ne interrogating laser and an optical configuration that will be described elsewhere.

Deaeration. Samples were depleted of O_2 in 5–10 min by the combination of argon flow through the tightly fitting Teflon stopper of the cuvette and the repeated displacement of the liquid with a Teflon cylindrical piston mounted on a rod through the stopper. This procedure is gentle and effective.

Data Analysis. The experimental records consisted of two contiguous data segments of 512 channels each representing the two polarized emission components $I_\parallel$ and $I_\perp$ as a function of time, t. The computerized data were processed by using a data editor written by Leon Avery. The pretrigger segments that supply the zero baseline were stripped and the records were combined so as to form the functions $S(t) = I_\parallel(t) + 2I_\perp(t)$ and $r(t) = [I_\parallel(t) - I_\perp(t)]/S(t)$. $S(t)$ represents the polarization-independent total emission intensity and $r(t)$ is the emission anisotropy (3, 4). The triplet lifetimes are derived by analysis of the former function and the rotational correlation times from the latter. For a hydrated sphere with a unique rigidly attached chromophore

$$S(t) = I_o e^{-t/\tau} \text{ and } r(t) = r_o e^{-t/\phi}, \quad [1]$$

in which I_o is the initial phosphorescence intensity, τ is the phosphorescence lifetime, r_o is the limiting anisotropy determined by the angle λ between the absorption and emission transition moments

$$r_0 = (3\cos^2\lambda - 1)/5, \quad [2]$$

and ϕ is the rotational correlational time related to the rotational diffusion constant D and thus to molecular volume V of the sphere and viscosity η of the medium according to

$$\phi = 1/6D = V\eta/kT = M_r(\bar{v} + h)\eta/RT, \quad [3]$$

in which k is the Boltzmann constant, R is the gas constant, T is the absolute temperature, M_r is the molecular weight, $\bar{v}$ is the partial specific volume, and h is the degree of hydration. For H_2O, 20°C, $\bar{v} = 0.73$ and $h = 0.2$ ml/g, $\phi = 0.38$ ns/kilodalton. Experimental values are characteristically 1.6 times higher (3, 18). Thus, we use

$$\phi_{exp} \approx 0.6 \text{ ns/kilodalton·cP}. \quad [4]$$

The expressions for $S(t)$ and $r(t)$ are more complex in the event of nonspherical rotors (3, 4, 19, 20), heterogeneity in chromophore orientation (3, 4, 19, 21), and anisotropy of the supporting medium or stereochemical restrictions to rotation (11, 19–21).

The $S(t)$ and $r(t)$ functions were analyzed independently in terms of up to two exponential components and one time in variant component with a nonlinear least squares program developed by Leon Avery. Deconvolution of the records was not required because the data were recorded in time ranges much longer than the exciting flash (5 ns).

RESULTS AND DISCUSSION

Photophysical Properties of Eosin. The singlet and triplet states of free and protein-bound eosin are well characterized (refs. 18 and 22–25 and references therein; triplet state spectroscopy is reviewed in refs. 26–28). The fluorescence and phosphorescence emissions occur at 560 and 690 nm, respectively (23). Other reported parameters at room temperature (collected from refs. 23–25) are (*i*) H_2O: $\Phi_f = 0.2$, $\tau_f = 0.9$ ns, $\Phi_{isc} = 0.7$, $\tau_p = 1.8$ ms, k_i (self-quenching by the ground state S_0) = $3–4 \times 10^8$ M^{-1} s^{-1}; (*ii*) glycerol: $\Phi_f = 0.4$, $\Phi_{isc} = 0.6$, $\Phi_p = 0.01$, $\tau_p = 2.6$ ms, in which Φ_f and τ_f are the fluorescence quantum yield and lifetime, Φ_{isc} is the intersystem crossing quantum yield, and Φ_p and τ_p are the phosphorescence quantum yield and lifetime.

We have measured the decay of the triplet state of aqueous solutions of the reagent EITC by both triplet–triplet absorption and phosphorescence emission, using the instrument shown in Fig. 1. The quality of the emission curves (Fig. 2A) is clearly superior to that obtained by absorption despite the 20-fold difference in concentration. [It should be noted, however, that in the case of eosin the transient signals are an order of magnitude larger by ground state depletion than by triplet–triplet absorption (18, 22).] The inherently greater sensitivity of phosphorescence (i.e., emission) measurements at low concentration derives from the square root dependence of the signal-to-noise ratio on concentration as opposed to the first power dependence in the case of absorption (12). The triplet

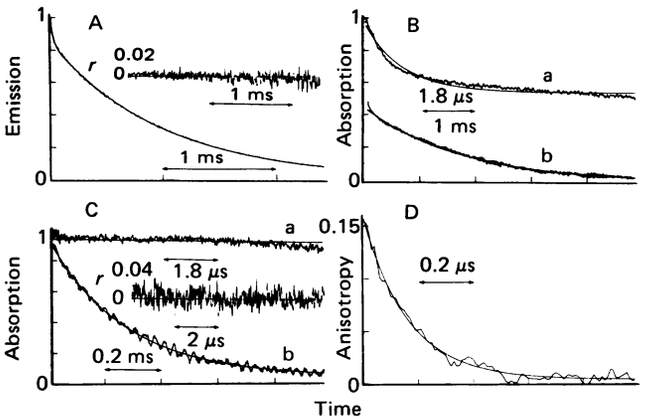

FIG. 2. Decay of the triplet state of EITC by phosphorescence and triplet–triplet absorption. (*A*) Emission of 0.5 μM EITC in P_i/NaCl. Average of 320 sweeps. The corresponding anisotropy *r* is shown as an *Inset*. (*B*) Absorption and corresponding anisotropy of 10 μM EITC in P_i/NaCl. Average of 1000 sweeps. (*C*) Same as *B* but in 80% glycerol. (*D*) Absorption anisotropy decay corresponding to *C*. All experiments were at 4°C. In panels with two curves (a, b), the data are temporally contiguous but are shown with different resolution. The smooth lines in this and other figures represent the results of computer analyses (Table 1).

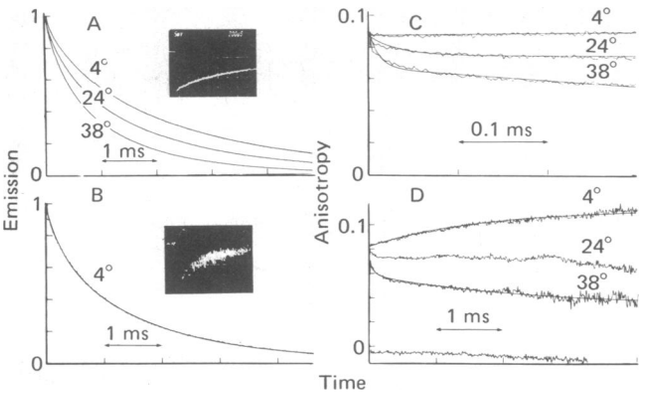

FIG. 3. Phosphorescence intensity and anisotropy kinetics of eosin-labeled human erythrocyte ghosts. (*A*) Emission of suspension with 2 μM eosin at three temperatures (all temperatures are °C). Average of 320 sweeps, one of which is shown in the *Inset*. (*B*) Same as in *A* but diluted with P_i/NaCl to 20 nM eosin. (*C* and *D*) Time course of emission anisotropy corresponding to data in *A* obtained with two degrees of temporal resolution. The lower horizontal curve in *D* represents data obtained with a horizontally polarized laser flash, which ideally should produce zero emission anisotropy.

lifetimes measured in water (Table 1) were compatible with literature values and give evidence for diffusion-controlled quenching by the eosin ground state (25) and possibly triplet–triplet annihilation at the higher concentrations used in absorption. In 80% (vol/vol) glycerol, both methods of measurement yielded similar long decay components but an additional faster process was resolved by absorption, the source of which is not known [under certain circumstances, the photochemistry and thus excited state kinetics of eosin can be quite complex (24, 25)]. Important controls for the accuracy of the system in the determination of emission anisotropy are given by the *insets* to Fig. 2 *A* and *B*; the controls show that the anisotropy function *r* was centered about 0, indicative of complete depolarization. In glycerol, however (Fig. 2*D*), a decay in linear dichroism was resolved with a ϕ of about 0.1 μs, a value compatible with Eq. 4. The $r(0)$ of 0.16 agrees well with data of Cherry and Schneider for eosin-labeled proteins in glycerol (18) but may be too low depending upon the as-yet-undetermined extent of ground state depletion (18, 22).

Eosin-Labeled Human Erythrocytes: The Band 3 Anion Transport System. The band 3 glycoprotein responsible for anion transport spans the erythrocyte membrane (for a review see ref. 30) and can be labeled with considerable specificity (>80%; refs. 14, 31, and 32) by EITC. The system has been investigated extensively by Cherry *et al.* (11, 14, 31–33), using transient dichroic absorption changes coupled to the triplet state. We have measured the decay of phosphorescence emission from human erythrocyte ghosts labeled externally by EITC as a function of temperature (Fig. 3*A*). The curves were decomposed into two components, the second of which got longer

Table 1. Summary of phosphorescence emission (Phos) and triplet–triplet absorption (Abs) decay parameters*

Compound	Conc., μM	Condition	Temp., °C	Signal	Lifetime $S(t)$ α_1	τ_1, μs	α_2	τ_2, ms	Anisotropy $r(t)$ β_1	ϕ_1, μs	β_2	ϕ_2, ms	$r(0)$
EITC	0.5	P_i/NaCl	4	Phos	0.14	27	0.86	1.0†					
	10	P_i/NaCl	4	Abs	1	270†							
	10	80% glycerol	4	Abs	0.49	1	0.51	1.7	0.16	0.14			
EITC-erythrocytes	2	5 mM $NaPO_4$, pH 7.3	4	Phos	0.17	320	0.83	2.2			−0.03	1.6	0.09
	2		24	Phos	0.28	370	0.72	1.9	0.01	30			0.09
	2		38	Phos	0.34	310	0.66	1.4	≈0.01	40 ± 30	0.02	2.3	0.09
	0.02		24	Phos	0.25	260	0.75	1.6					
Eosin-Con A	1–2	Buffer‡	4	Abs	0.28	45	0.72	0.73					
	1–2	Buffer‡	4	Phos	0.35	55	0.65	0.69					
	1–2	Buffer‡ + 0.1 M MeMan	4	Phos	0.31	68	0.69	0.45					
	0.5	98% glycerol¶	4	Phos	0.19	61	0.81	1.6	0.03	§	0.04	0.14	0.08
	2	100% glycerol¶	4	Abs	0.10	2	0.90	1.2	0.05	2	0.07	0.34	0.12
	≈0.1	Bound to F4N	4	Phos	0.46	22	0.54	0.35	≈0.05	∞			0.06
		Friend cells	37	Phos	0.57	15	0.43	0.21	≈0.04	∞			0.05

* Data primarily from Figs. 2–5. Lifetime amplitudes (α_i) are given as fractional contributions to the total decay. The anisotropy amplitudes (β_i) are in absolute units. The $r(0)$ values have been corrected by the factor 1.14, which accounts for the large emission aperture (29).

† Assuming that these differences are due to the concentration dependence of ground state quenching (25), a value for $k_i = 3 \times 10^8\ M^{-1}\ s^{-1}$ results.

‡ The buffer was 10 mM KPO_4, pH 7.4/0.3 M NaCl/1 mM $MgCl_2$/1 mM $CaCl_2$. MeMan, methyl α-D-mannopyranoside.

§ Too fast for the apparatus in the phosphorescence detection mode.

¶ Nominal values. The true concentrations may have been up to 2% lower due to hydration.

and increased in relative amplitude as the temperature was reduced (Table 1). The lifetimes of triplet probes complexed or conjugated to proteins are characteristically multiple and shorter than those of the free chromophores (refs. 18, 25, and 32; see also below).

The sensitivity of the phosphorescence detection technique is demonstrated by data accumulated at a 20 nM concentration of the probe (Fig. 3*B*). A comparison of the single traces depicted in the *insets* of Fig. 3 *A* and *B* reveals the expected difference in signal-to-noise ratio (theoretically 10-fold) for the 100-fold change in concentration. The dramatic effect of signal averaging on the quality of the cumulative decay curves is evident.

The time-resolved emission anisotropies corresponding to the experiments of Fig. 3*A* are shown in Fig. 3 *C* and *D* with different temporal resolution. In all cases, a finite anisotropy was observed at the longest measurable time (3–4 msec). This finding indicates that rotational relaxation in this system is anisotropic and restricted and is consistent with the linear dichroism measurements of Cherry and his colleagues. The anisotropy at $t = 0$ of 0.09 was invariant with temperature and if equated to r_o (Eq. 2) corresponds to an angle of 46° between the singlet absorption and apparent triplet emission transition moments. (This estimate of r_o may be too low, however, if the polarization varies across the emission band or if there is appreciable independent motion of the probe.) The emission is predominantly polarized in-plane as judged by the positive value of r_o, a result consistent with the known perturbing effects of heavy atom substituents on the π–π^* triplet state of aromatic molecules (26–28).

The time courses of phosphorescence anisotropy at the three temperatures (Fig. 3) were significantly different. Thus, at 4°C the anisotropy actually increased with time, at room temperature it decreased slightly, and at 38°C it decreased more significantly. The observed behavior was not due to irreversible structural changes, as was evidenced by reversibility with a given sample exposed to bidirectional shifts of temperature. The apparent and predominant rotational correlation times were in excess of 1 msec (Table 1), but at 38°C there existed indications for decay of anisotropy in the range of 10–100 μsec. The results are consistent with the notion that the molecular entity sensed by the eosin probe has a more rigid structure as the temperature decreases, and it is interesting that the transport function of band 3 is markedly temperature dependent in the range tested (30).

A more quantitative statement depends upon the molecular model adopted for the system. For example, assuming that band 3 can be represented as a rigid ellipsoid of revolution (4, 11, 19, 31), the curve at 4°C would imply that the absorption and emission transition moments more or less straddle the rotation axis. [The minimal condition for negative amplitudes in the decay of anisotropy (Eq. 5) is that the angle between the projections of the absorption and emission transition moments on the plane normal to the axis of symmetry and rotation be greater than 45°. For a related case, see ref. 34.] As the temperature increases, segmental elastic deformation or more global conformation change generates additional relaxation modes that lead to a greater contribution of out-of-plane relative to in-plane rotation (20) and thus ultimately to a net depolarization. An alternative interpretation based upon the concept of diffusion within a cone of restricted motion (21) would be that the angular constraints diminish with temperature. It should be added that a ϕ of 1–2 ms is not consistent with Eq. 4 (i.e., is too large) when the reported values of 3–10 P are used for the microviscosity of the erythrocyte (ghost) membrane in the temperature range 37–10°C (35). Furthermore, the values obtained by transient linear dichroism are not affected by spectrin depletion [at neutral pH; at low pH, the aggregation of intramembrane particles is favored and rotation is hindered (31)] or by chemical crosslinking (33), procedures that should modify the external, internal, and lateral (with respect to the membrane) interactions of band 3 molecules. Thus, one conclusion might be that the observed slower depolarization derives from the concerted motion of larger aggregates of band 3 or complexes with other as-yet-undefined components of the membrane. It is also possible that the faster relaxations at 38°C seen in Fig. 3 might reflect discrete segmental motions associated with ion translocation (30).

During the preparation of this manuscript, additional data from Nigg and Cherry were reported on the dichroic absorption kinetics of band 3 labeled with eosin-maleimide (32). These authors also found temperature-dependent triplet lifetimes and anisotropy decays similar to those of Fig. 4. However, the increase in r seen at 4°C by phosphorescence was not observed in absorption, as is expected because the latter measurement uses the same electronic transition for the actinic and interrogating processes.

Eosin-Con A. The binding of the lectin Con A to the surface glycoproteins and glycolipids of eukaryotic cells produces a number of effects, including agglutination, mitogenic stimulation, and redistribution (6) and anchorage modulation (8) of surface receptors. The increased agglutinability of malignant and transformed compared to normal cells has been ascribed in part to enhanced mobility of the lectin receptors (see ref. 9). There exists evidence based on steady state fluorescence polarization data for the differential rate of rotation of Con A bound to normal and malignant cells (36). However, measurements of the lateral diffusion of lectin receptors have demonstrated that the latter are relatively immobile (7).

In the present study, we examined the rotational properties of bound Con A by using the phosphorescence anisotropy approach. Con A was labeled with EITC and characterized by time-resolved phosphorescence emission (Fig. 4 *A* and *B*) and triplet–triplet absorption (Fig. 4 *C* and *D*). The two methods of detection (Fig. 4 *A* and *C*) yielded decay parameters in fairly good agreement (Table 1). The addition of methyl α-D-mannopyranoside, a specific monosaccharide ligand for Con A, led to a shortening of the slower component, a finding which suggests that triplet lifetimes may be useful for studies of ligand interactions. At least two components were also observed in the decay of anisotropy. In the latter case, the values for the rotational times were consistent with those predicted for the global

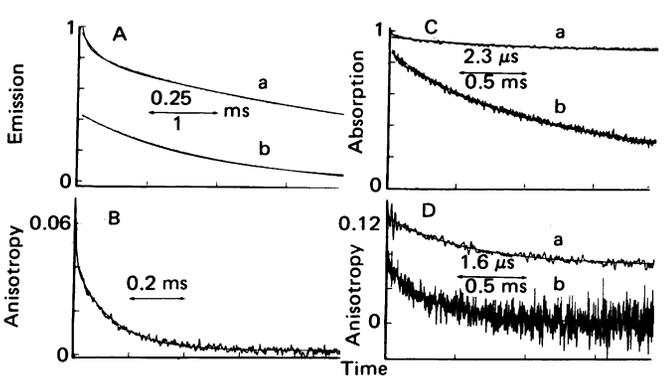

FIG. 4. Triplet decay by phosphorescence and triplet–triplet absorption of eosin-Con A in glycerol. (*A* and *B*) Emission intensity and anisotropy of a 0.5 μM (in eosin) solution at 4°C in 90% glycerol. Average of 320 sweeps. (*C* and *D*) Absorption and absorption anisotropy of a 2 μM solution at 4°C in 100% glycerol. The curves a and b are defined in Fig. 2.

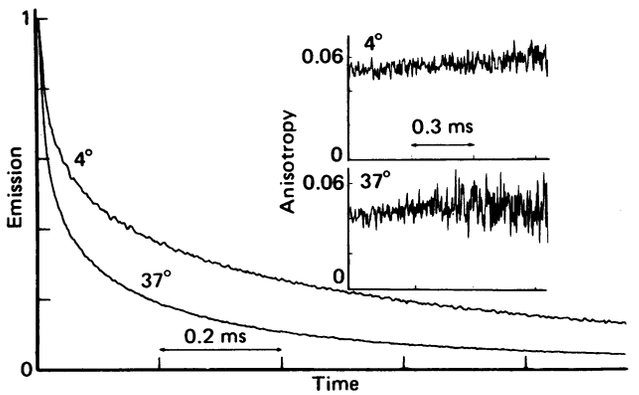

FIG. 5. Phosphorescence intensity and anisotropy decay kinetics of Friend cells labeled with eosin-Con A. Average of 1280 sweeps.

rotation of an equivalent sphere (Eq. 4). The second, smaller, rotational correlation time seen by absorption (but not emission due to the more limited temporal range of the latter) we attribute to local motion of the probe.

Cells Labeled with Eosin-Con A. We examined the rotational mobility of eosin-Con A bound to mouse spleen cells transformed with Friend erythroleukemia virus. These cells can be induced to resume erythroid differentiation by exposure to chemical agents *in vitro* (16). During this process, the number of Con A binding sites (*ca.* $1\text{–}2 \times 10^7$ per cell) and cellular agglutinability change significantly (17). The lectin receptors appear to be in close proximity according to fluorescence energy transfer experiments (15).

The phosphorescence properties of suspensions of cells labeled with eosin-Con A are depicted in Fig. 5. The triplet lifetimes were significantly shorter than those seen for the probe alone (Table 1) and perhaps reflect an accentuation of the effect seen with the monosaccharide ligand. The striking finding was the absence of a perceptible decay in the phosphorescence emission anisotropy at either 4°C or 37°C. We conclude that there is no significant global rotation of bound Con A (and by implication of the corresponding receptors) under the conditions of this experiment (preliminary data indicate that this result may be generalizable to other cells and dimeric Con A). However, the anisotropies at $t = 0$ in Fig. 5 are lower than those observed with the protein in glycerol or with eosin-labeled membranes (Table 1). It is quite probable that the local motion of the eosin probe resolved in Fig. 4*D* by absorption (and partially by phosphorescence) is too rapid for detection in the measurement on cells suspended in aqueous media. One explanation for the apparent discrepancy between our results and those obtained by steady-state fluorescence depolarization, therefore, would be that the latter method produces average values reflecting the contributions both of global and local motion.

By faster gating of the photomultiplier (or in the absence of fluorescence) the phosphorescence measurements described here can be extended into the nanosecond range so as to overlap with high-resolution fluorescence techniques (2–4, 37). Thus, the total polarized luminescence can provide information about rotational motion in the range of $\approx 10^{-10}$ to 1 second.

We are indebted to Dr. Richard Cherry for generous advice and for making available research results prior to publication. We are also grateful for assistance on the part of Dr. Robert Clegg in the design of the sample cuvette, Dr. Yusuf Tan in electronics and data analysis, Dr. Donna Arndt-Jovin in studies with cells, and numerous colleagues in the preparation of the manuscript. R.H.A. and S.S.C. were recipients of postdoctoral awards from the Max Planck Society.

1. Weber, G. (1953) *Adv. Protein Chem.* **8,** 415–459.
2. Weber, G. (1977) *J. Chem. Phys.* **66,** 4081–4091.
3. Yguerabide, J. (1972) *Methods Enzymol.* **26,** 498–578.
4. Wahl, P. (1975) in *New Tech. Biophys. Cell Biol.* **2,** 233–285.
5. Thomas, D. D. (1978) *Biophys. J.* **24,** 439–462.
6. Edidin, M. (1974) *Annu. Rev. Biophys. Bioeng.* **3,** 179–201.
7. Schlessinger, J. & Elson, E. L. (1979) in *Biophysical Methods,* Methods of Experimental Physics, eds. Ehrenstein G. & Lecar, H. (Academic, New York), in press.
8. Edelman, G. M. (1976) *Science* **192,** 218–226.
9. Bell, G. I. (1978) *Science* **200,** 618–627.
10. Naqvi, K. R., Gonzalez-Rodriguez, J., Cherry, R. J. & Chapman, D. (1973) *Nature (London) New Biol.* **245,** 249–251.
11. Cherry, R. J. (1978) *Methods Enzymol.* **54,** 47–61.
12. Rigler, R., Rabl, C.-R. & Jovin, T. M. (1974) *Rev. Sci. Instrum.* **45,** 580–588.
13. Vaz, W. L., Austin, R. H. & Vogel, H. (1979) *Biophys. J.* **26,** 415–426.
14. Nigg, E., Kessler, M. & Cherry, R. J. (1979) *Biochim. Biophys. Acta* **550,** 328–340.
15. Chan, S. S., Arndt-Jovin, D. J. & Jovin, T. M. (1979) *J. Histochem. Cytochem.* **27,** 56–64.
16. Dube, S. K., Pragnell, I. B., Kluge, N., Gaedicke, G., Steinheider, G. & Ostertag, W. (1975) *Proc. Natl. Acad. Sci. USA* **72,** 1863–1867.
17. Eisen, H., Nasi, S., Georgopoulos, C. P., Arndt-Jovin, D. J. & Ostertag, W. (1977) *Cell* **10,** 689–695.
18. Cherry, R. J. & Schneider, G. (1976) *Biochemistry* **15,** 3657–3661.
19. Rigler, R. & Ehrenberg, M. (1976) *Q. Rev. Biophys.* **9,** 1–19.
20. Shinitzky, M., Dianoux, A.-C., Gitler, C. & Weber, G. (1971) *Biochemistry* **10,** 2106—2113.
21. Kinosita, K., Jr., Kawato, S. & Ikegami, A. (1977) *Biophys. J.* **20,** 289–305.
22. Cherry, R. J., Cogoli, A., Oppliger, M., Schneider, G. & Semenza, G. (1976) *Biochemistry* **15,** 3653–3656.
23. Parker, C. A. & Hatchard, C. G. (1961) *Trans. Faraday Soc.* **57,** 1894–1904.
24. Kasche, V. & Lindqvist, L. (1965) *Photochem. Photobiol.* **4,** 923–933.
25. Fisher, G. J., Lewis, C. & Madill, D. (1976) *Photochem. Photobiol.* **24,** 223–228.
26. McGlynn, S. P., Azumi, T. & Kinoshita, M. (1969) *Molecular Spectroscopy of the Triplet State* (Prentice Hall, Englewood Cliffs, NJ).
27. Lower, S. K. & El-Sayed, M. A. (1966) *Chem. Revs.* **66,** 199–241.
28. Turro, N. J., Liu, K.-C., Chow, M.-F., & Lee, P. (1978) *Photochem. Photobiol.* **27,** 523–529.
29. Jovin, T. M. (1979) in *Flow Cytometry and Sorting,* eds. Melamed, M., Mullaney, P. & Mendelsohn, M. (John Wiley, New York), pp. 137–165.
30. Cabantchik, Z. I., Knauf, P. A. & Rothstein, A. (1978) *Biochim. Biophys. Acta* **515,** 239–302.
31. Cherry, R. J., Burkli, A., Busslinger, M., Schneider, G. & Parish, G. R. (1976) *Nature (London)* **263,** 389–393.
32. Nigg, E. A. & Cherry, R. J. (1979) *Biochemistry* **18,** 3457–3465.
33. Nigg, E. A. & Cherry, R. J. (1979) *Nature (London)* **277,** 493–494.
34. Harvey, S. C. & Cheung, H. C. (1977) *Biochemistry* **16,** 5181–5187.
35. Cooper, R. A. (1978) *J. Supramol. Struct.* **8,** 413–430.
36. Inbar, M., Shinitzky, M. & Sachs, L. (1973) *J. Mol. Biol.* **81,** 245–253.
37. Munro, I., Pecht, I. & Stryer, L. (1979) *Proc. Natl. Acad. Sci. USA* **76,** 56–60.